

UNSTEADY NUMERICAL SIMULATION OF TURBULENT FORCED CONVECTION IN A RECTANGULAR PIPE PROVIDED WITH WAVED POROUS BAFFLES

F. Fakiri¹, K. Rahmoun²

ABSTRACT

Numerical simulations of flow and heat transfer in a serpentine heat exchanger configuration are presented to demonstrate application of porous media techniques in heat exchanger analyses. In this study, steady-state 3D turbulent forced convection flow and heat transfer characteristics in a rectangular pipe with baffles attached inside pipe have been numerically investigated under constant wall heat flux boundary condition. Numerical study has been carried out for Reynolds number of 20000-50,000, Prandtl number of 0.71, baffle distances h/D_h of 1/3 and 2/3, and baffle thickness e of 1/12, 2/3. It is observed that rectangular pipe having waved baffles has a higher Nusselt number and friction factor compared to the smooth rectangular pipe without baffles. Periodically fully developed conditions are obtained after a certain module. Maximum thermal performance factor is obtained for the baffle waved. Results show that baffle distance, waved porous baffle, and Reynolds number play important role on both flow and heat transfer characteristics. All the numerical results are correlated within accuracy of $\pm 2\%$ and $\pm 2.5\%$ for average Nusselt number and friction factor, respectively.

Keywords: Porous media, Horizontal Canal, Thermal transfer and matter, Model Darcy-Brinkman-Forchheimer, Forced convection, Porous baffles.

INTRODUCTION

Heat transfer from a surface is increased with increasing convection heat transfer coefficient or increasing heat transfer surface area. In order to enhance the heat transfer coefficient, a pump or fan is used, or existing one is replaced with a larger one; however, it may or may not be convenient. Another method to increase the heat transfer from a surface is to increase the surface area. Heat transfer surface area may be increased using baffles or fins on the surfaces of the ducts. Turbulent flows in rectangular pipes are encountered in many engineering applications such as nuclear reactors, shell and tube heat exchangers, cooling of gas turbines and combustion chambers, and cooling of electronic devices [1]. Turbulent flows in rectangular channels are encountered in many engineering applications such as nuclear reactors, shell and tube heat exchangers, cooling of gas turbines and combustion chambers, cooling of electronic devices and air solar collector. Turbulent flow and heat transfer in rectangular conducts have been studied by a number of investigators. Turbulent flow and heat transfer for tubes and annuli with longitudinal internal baffle were analyzed by Yue-Tzu Yang, Chih-Zong Hwang [2]. Nicolau B. Santos et al. [3] examined the effect of entrance condition on forced convection heat transfer in a channel porous baffles. Kang-Hoon Ko, N.K. Anand [4] experimentally investigated to determine the detailed module-by module pressure drop characteristics of flow inside rectangular channels. Yang et al. [5], we performed a comprehensive numerical study on forced convection heat transfer in three-dimensional 3D porous pin fin channels with air as the cold fluid. Nabila Targui, Henda Kahalerras [6] numerically studied 2D turbulent flow through a rectangular conduct with baffle attached circumferentially. P.C. Hvang and K. vafait [7] numerically investigated 2-D turbulent flow and heat transfer in channel using porous blocks. H. Benzenine, et al. [8] carried out a numerical study to study airflow and heat transfer in a channel with waved fins. Tandiroglu and Ayhan [9] experimentally investigated the energy dissipation analysis of transient forced convection heat transfer in a pipe with baffles inside the duct.

According to this literature review, we note that little works have been devoted to studies of the effects of the waved porous fins and/or porous baffles on the flow of heat transfer in heat exchangers. The objective in this paper is to quantify numerically the heat transfer by forced convection for different velocities of flow and analyze the geometrical and physical effects of the corrugated fins on heat transfer. A survey of the literature reveals the lack of information on steady-state 3D forced convection turbulent heat transfer and pressure drop for rectangular channel with waved porous fins. In this study, the characteristics of a steady-state 3D turbulent flow and heat

This paper was recommended for publication in revised form by Regional Editor Mohamed Awad

¹Department of Physics, Faculty of Science, Research Unit Materials and Renewable Energies U.R.M.E.R, University Abou Bekr Belkaid, BP 119, 13000 Tlemcen, Algeria

**E-mail address: docfakiri_etsmerauto@yahoo.fr, k_rahmoun@yahoo.fr*

Manuscript Received 9 June 2016, Accepted 3 September 2016

transfer in a rectangular conduct with porous baffles are investigated numerically using commercial software Ansys Fluent 12.3.26. under constant wall heat flux boundary condition. Standard k- ϵ turbulence model is used to simulate flow. The effects of Reynolds number, baffle distance, and baffle angle on fluid flow and heat transfer are examined. The results of this investigation are hoped to provide numerical data for 3D turbulent convective heat transfer in complex geometries.

Material

The porous medium may be defined as a material consisting of a solid matrix with a gap between them. Kaviany [10] has classified the matrix structures of porous media based on the structural characteristics of porous media. The porous media where the grains are not connected to each other are considered blocks. If the grains are cemented together as solid matrices are called consolidated porous media. Extensive reviews can be found in several books [11-12]. Darcy showed in his experiment that the mass flow is proportional to the pressure drop and inversely proportional to the length of the test section. The effort has been put into many studies to obtain the methods of evaluation of permeability.

Since Darcy's model is not valid when the flow velocity is relatively high, Forchheimer suggested that the square of the velocity may better reflect the inertial type of drag force. He introduced the Forchheimer-Extended Darcy model by adding the inertial drag. When the flow has constraints such as a wall, there is a sharp drop in the flow velocity due to the effects of the wall. Brinkman incorporated this effect by adding the Brinkman term. While Wooding [13] was the first who applied the Darcy model to convective terms, Vafai and Tien [14] suggested macroscopic governing equations derived from Navier-Stokes' equations using Slattery's [15, 16] volume average method and the Brinkman-Forchheimer-Extended Darcy model. Vafai and Tien, at this time, used the pore velocity as the variable of the Brinkman-Forchheimer Extended Darcy term. Later, Hunt and Tien [17] suggested another type of governing equation using the Darcian velocity, which was the basis for most of the research papers. Nakayama [18] suggested that pore-pressure should be used for the momentum equation since the pressure can be gauged only inside the pore region. Many studies quoted the governing equation for the flow in porous media, which was developed by Vafai and Tien [14] for their numerical simulations, but these studies often used slightly modified types of equations.

The present work the material used for porous baffle is an aluminum foam material manufactured using a process patented by ERG Aerospace Inc., CA whereas in the previous case [4] porous baffles were made of sintered bronze beads. In Figure 1.

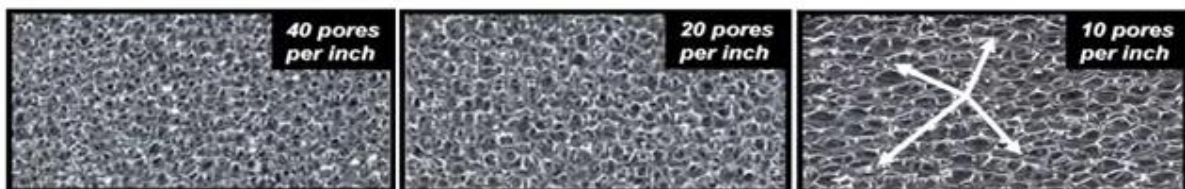


Figure 1. Samples of the porous material [4].

Thus the scope of the present study is very different than that of Hwang [4]. The main aim of this study is to find the most convenient location for a floating renewable energy platform. For this reason, five different regions were selected to analyze and to be able to make a comparison, the power data of the different energy types were converted to the same unit and the regions were ranked with respect to these results.

Mathematical Formulation

The geometry of the problem is presented on Figure. 2. The system consists of air flow moving through a rectangular channel provided with porous baffles. Two different forms of baffles are analyzed; a first form is plate porous baffle Figure. 2-b and a second form waved porous baffle Figure. 2-c.

The coordinate system, the computational domain and the geometric characteristics are presented in the following Figure. Computational domain consists of three consecutive parts: 1,2192 m in length entrance section L_e , 1,0668 m in length test section L_c and 0,308 m in length exit section L_s .

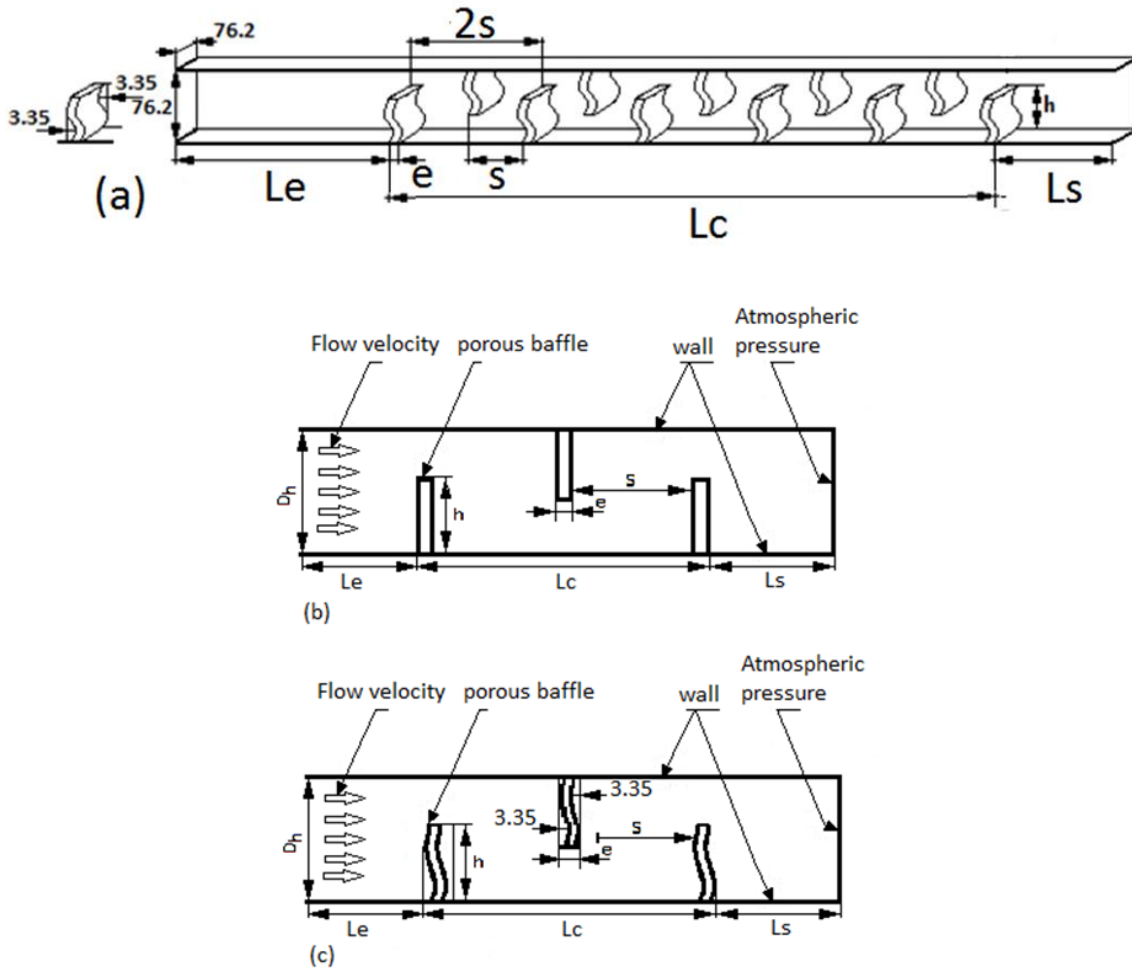


Figure 2. Rectangular pipe with waved porous baffle

The principle flow is in the X-direction. In figure. 2-a, s is the baffle distance, L_e is the length of the entrance section, L_c is the length of the test section, L_s is the length of the exit section, e represents the porous baffle thickness, h the baffle height, and D_h the diameter of the rectangular pipe. Shaded area consisting of three baffles shown in figure. 2-c is called module.

Field of Study

The general transport equation that describe the principle of conservation of mass and momentum can be written in the following conservative form Patankar [4]. The flow field is compressible, stable, isothermal turbulent flow. In a Cartesian system continuity den formed tensor equation is:

$$\frac{\partial \rho}{\partial t} = \vec{\nabla} \cdot (\rho \vec{v}) = 0 \quad (1)$$

Momentum equation of compressible viscous fluid motion is as follows:

$$\rho \left[\frac{\partial \vec{v}}{\partial t} + (\vec{v} \cdot \vec{\nabla}) \vec{v} \right] = -\vec{\nabla} P_1 + \mu \left[\nabla^2 \vec{v} + \frac{1}{3} \vec{\nabla} (\vec{\nabla} \cdot \vec{v}) \right] + \rho \vec{f} \quad (2)$$

$$\rho c_p \left(\frac{\partial T}{\partial t} + \vec{v} \cdot \vec{\nabla} T \right) - \left(\frac{\partial P}{\partial t} + \vec{v} \cdot \vec{\nabla} P \right) = \tau \quad (3)$$

Standard k-ε equation turbulence model in jet simulation [19].

$$\frac{\partial(\rho k)}{\partial t} + \frac{\partial(\rho k u_i)}{\partial t} = \frac{\partial}{\partial x_i} \left[\left(\mu + \frac{\mu_t}{\sigma_k} \right) \frac{\partial k}{\partial x_j} \right] + G_k - \rho \varepsilon \quad (4)$$

$$\frac{\partial(\rho \varepsilon)}{\partial t} + \frac{\partial(\rho \varepsilon u_i)}{\partial t} = \frac{\partial}{\partial x_i} \left[\left(\mu + \frac{\mu_t}{\sigma_k} \right) \frac{\partial \varepsilon}{\partial x_j} \right] + \frac{c_{1\varepsilon} \varepsilon}{k} G_k - c_{2\varepsilon} \rho \frac{\varepsilon^2}{k} \quad (5)$$

$$\mu_t = \rho c_\mu \frac{k^2}{\varepsilon} \quad (6)$$

$$c_{1\varepsilon} = 1.44, c_{2\varepsilon} = 1.92, c_\mu = 0.09, \sigma_R = 1.0, \sigma_k = 1.3$$

Turbulent flows in the test section with a fully developed velocity profile and constant temperature. The 3D Navier-Stokes and energy equations are used to describe the flow and heat transfer in the computational domain. The 3D Incompressible Newtonian flow with the dissipation of energy by the viscous forces is negligible at steady state has been regarded as turbulent. Thermo-physical properties are assumed to be constant. Thus, the continuity equations, impulse, energy, and the standard k-ε turbulence model can be written as follows, respectively [20].

Numerical Approach

Numerical solutions are carried out using Ansys Fluent 12.3.26, a commercial finite volume- based CFD program. Turbulence is modeled employing the standard k-ε turbulence model with enhanced wall treatment, a near-wall modeling method that unites a two-layer model applicable in regions with fine near wall meshes with enhanced wall functions used in regions with coarse meshes [21]. Numerical simulations were tested by varying the number of elements of calculation. Stability and a convergence of the model reached for all the grids were assured. Non-structured grid elements with the quadrilateral type used because it considered being more adequate for the geometry suggested. The governing equations of our problem are solved by the finite volume method (FVM), based on the algorithm SIMPLEC (Patankar, 1980) [4]. The Reynolds averaged Navier-Stokes equations are solved numerically in conjunction with transport equations for turbulent flow. Near wall regions are fully resolved for $y^+ < 0.85$ in all the calculations. In the present study, non-uniform grids are employed for all numerical solutions performed. Typical mesh distribution on x-y-z for different waved porous baffle is represented in figure 3.

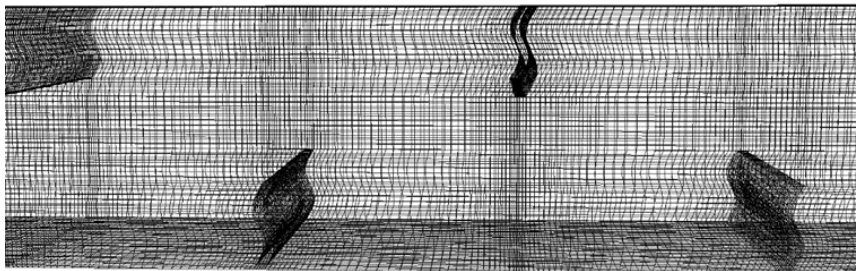


Figure 3. Representation of the distribution of the grid in the channel.

The grid independence study is performed by changing the mesh size inside the computational domain until the variation in velocity error are less than 0.021% and 0.023%, respectively (table.1). Steady segregated solver is employed with second order upwind scheme for convective terms in the mass, momentum, energy, and turbulence equations SIMPLE-algorithm. The choice of this mesh is justified by the fact that the difference between the values found is less than 1%.

For the numerical simulations presented in this work, we refer to the numerical and experimental work done by Kang-Hoon Ko, N.K. Anand [4] who studied the porous baffles with a plane shape.

Table 1. Comparison results for different mesh grids.

| GRILLE | 72×15×15 | 72×30×30 | 72×45×45 | 44×45×40 |
|------------------|----------|----------|----------|----------|
| X | 1,8288 | 1,8288 | 1,8288 | 1,8288 |
| Y | 0,0406 | 0,0406 | 0,0406 | 0,0406 |
| Z | 0,0381 | 0,0381 | 0,0381 | 0,0381 |
| ERROR | 0,02525 | 0,02259 | 0,0217 | 0,0288 |
| U _{max} | 5,863 | 5,953 | 5,991 | 5,982 |
| V _{max} | 2,037 | 2,227 | 2,233 | 2,234 |

A waved porous baffle is considered, and all the modeling conditions are inspired from the numerical study. Sensitivity analysis of the mesh and the numerical model validation are presented in this section, Figure 4.

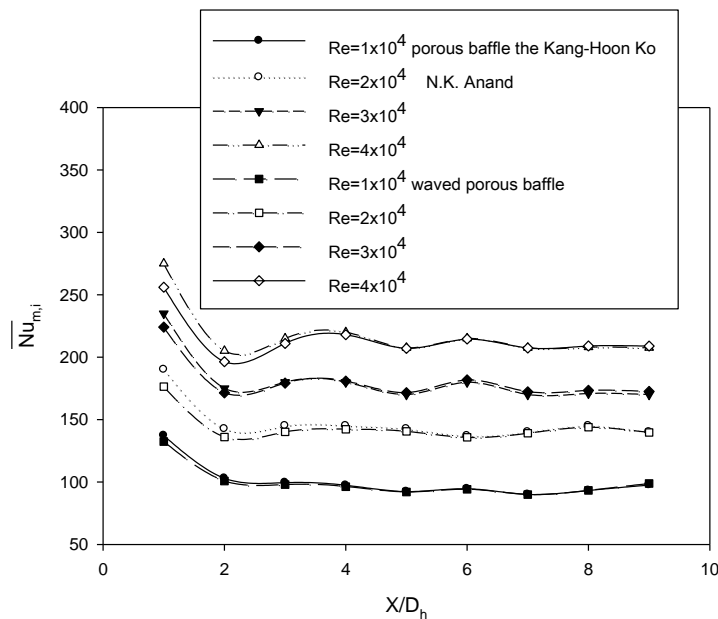


Figure 4. Average module Nusselt number between two forms transverse porous baffle and waved porous baffle $20PPI \ h / D_h = 1/3$.

Results and Discussion

Figure 5 shows the axial velocity contours for the different cases studied in this paper at $Re = 20 \cdot 10^4 \ h / D_h = 1/3$, $PPI = 20$. For rectangular porous baffles, Figure. 5-a is the same geometry studied by Kang-Hoon Ko, N.K. Anand [4], the other contours Figure. 5-b are those of waved baffles. It is indicating clearly that the values of velocity are very low in the vicinity of the porous baffles especially in the areas located downstream. This is characterized by the presence of the zones of re-circulation. One notices also the increased velocity in space between the tip of each porous baffle and the opposite walls of the channel. Dynamic configuration of the flow changes from one case to another, whatsoever with the change in the form of porous baffles or change the porosity.

In the first part, this increase is generated by the singularity represented by the obstacles and in the second part by the recirculation of the flow, which then brings about a sudden change in the direction of the fluid. It is also noted that the high-velocity values appear close to the high channel with an acceleration process which begins just after the second porous baffle.

In the first zone, located just upstream of the porous baffle, the fluid flow, comes with a constant velocity U_x . As we approach the first porous baffle, the current lines are deflected and the velocity profiles are more affected by it. The second area is located above the first fin and the air is accelerated by the effect of reducing the flow area.

The flow pattern is also affected by the porous structures height as it appears in Figure 6. Increasing h/D_h , when a porosity is kept at a constant value ($\epsilon=0.92$), leads to a distribution of the flow and the formation of a vortex behind each porous baffle. When these latter occupy the entire annular gap ($h/D_h = 2/3$), there is a

stabilization of the flow and the fluid moves in a fairly uniform fashion. The same behavior is observed when the waved porous baffle is attached in configuration Figure 6. The Collision area is reduced and the central region changes its orientation. It can be observed the formation of a recirculating flow whose extent is proportional to the Reynolds number. This phenomenon is illustrated by the negative values profile velocity in this area.

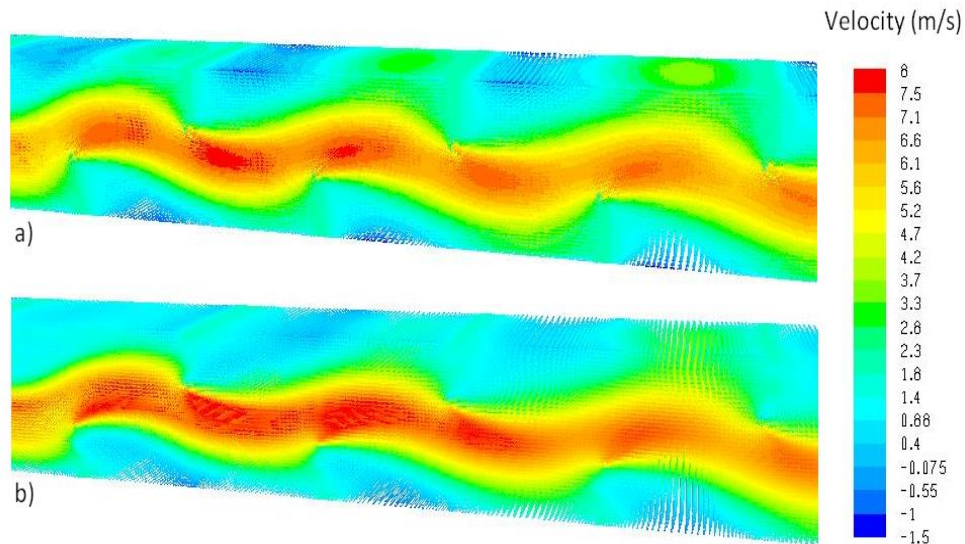


Figure 5. Axial velocity field in a conduct with waved porous baffle a) Transverse b) Waved for case ($Re = 20000$, $h / D_h = 1/3$, $PPI = 20$)

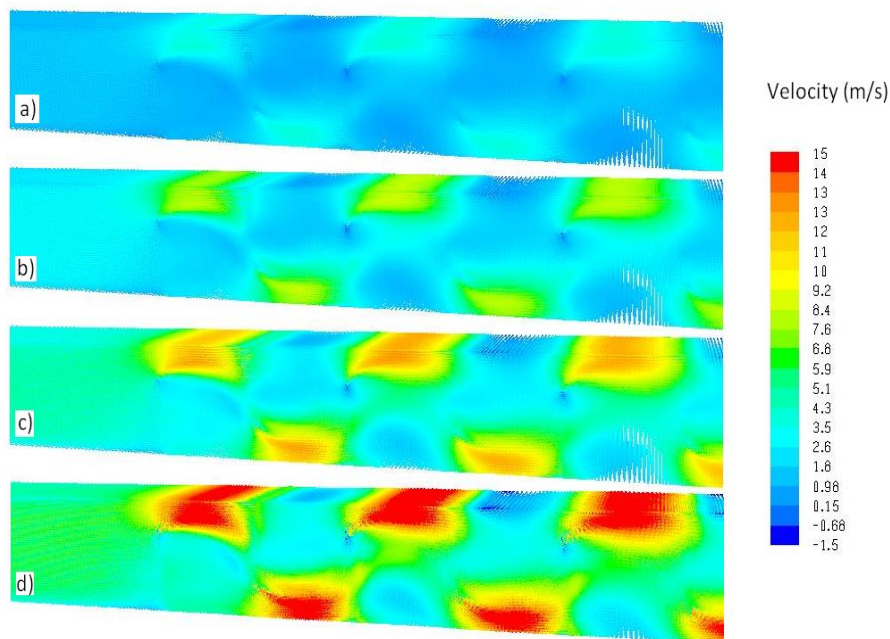


Figure 6. Axial velocity field in a conduct with Waved porous baffle a) 10000 b) 20000 c) 30000 and d) 40000) to $h / D_h = 2/3$, $PPI = 20$.

The flow in the test channel is thermally developing. Since for an asymmetric heated channel, the thermally developing is close to Kang-Hoon Ko, N.K. Anand [4] the last few copper blocks were averaged to get a good representation of the close to fully developed heat transfer. The fully developed Nusselt numbers and friction factors obtained in the present study for rectangular pipe with waved porous baffles are compared with

those given in the literature. Effect of the porous baffles geometry on the heat transfer rate is presented in the form of average Nusselt number and friction factor with Reynolds number as depicted in the Figures 7,8, 9 and 10.

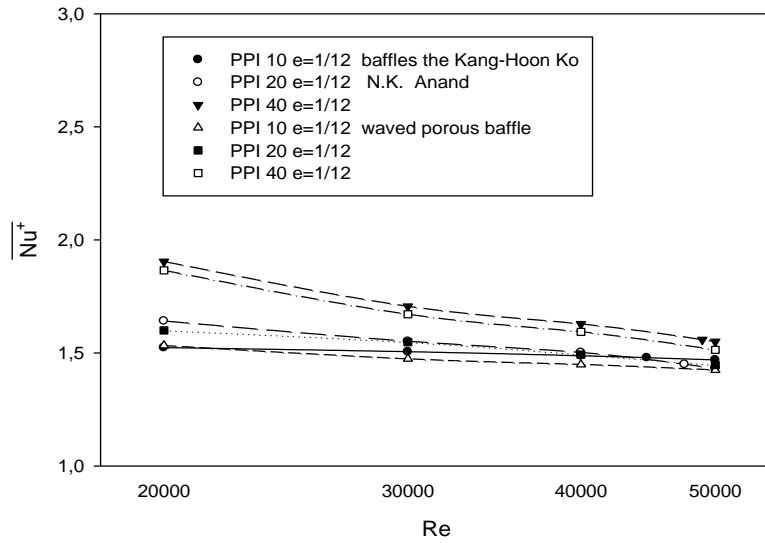


Figure 7. The heat transfer ratio for $h / D_h = 1/3$

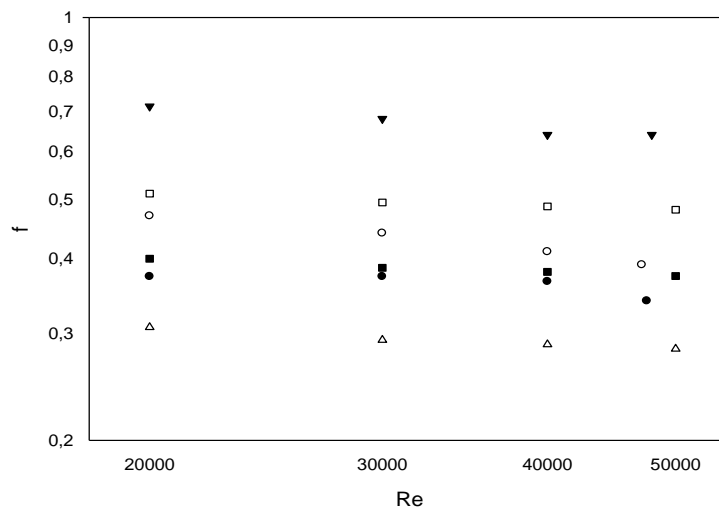


Figure 8. Coefficient of friction for $h / D_h = 1/3$

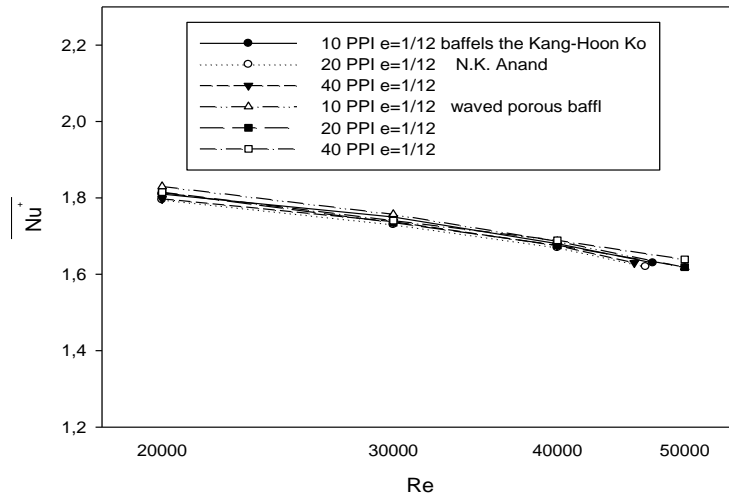


Figure 9. The heat transfer ratio for $h / D_h = 2/3$

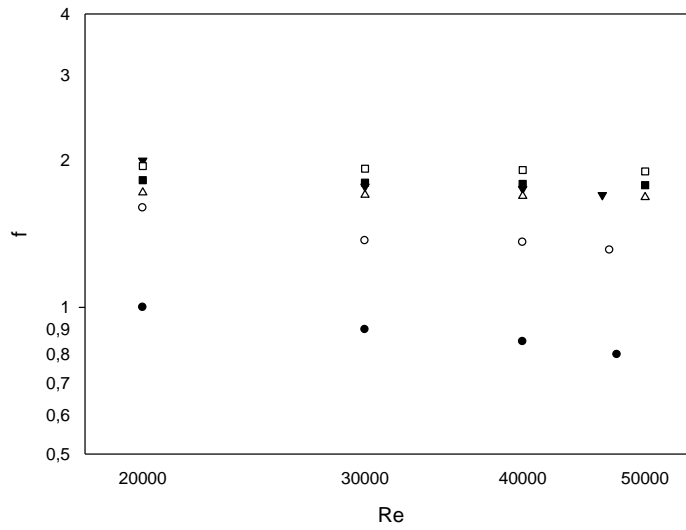
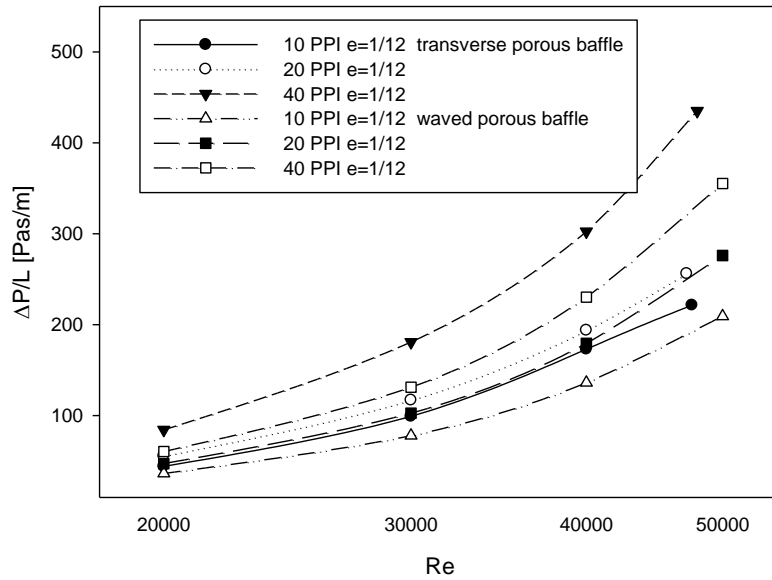
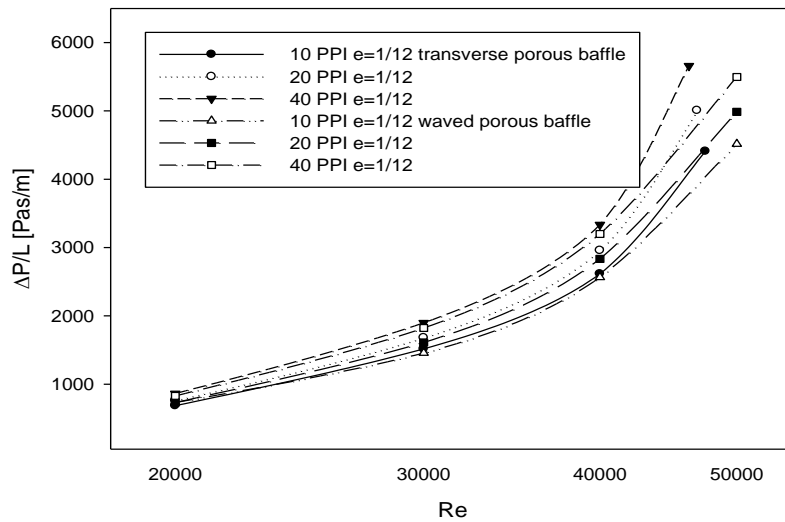


Figure 10. Coefficient of friction for $h / D_h = 2/3$



(a)



(b)

Figure 11. The pressure variation for (a) $h / D_h = 1/3$ and (b) $h / D_h = 2/3$

The numerical investigations of hydraulic performance in a rectangular conduct with waved porous baffle stepped of different pitch ratios, and stepped number are presented. According to the numerical analysis, obtained results are compared in this section. First of all, Nusselt number and the friction factor for numerical method are compared with experimental results of Kang-Hoon Ko, N.K. Anand [4].

Figures show comparison between the results of the present study and experimental data which implied above. There is a good agreement between the results for the present experimental method and numerical. Effect of the porous baffles geometry on the heat transfer rate is presented in the form of average Nusselt number and friction factor with Reynolds number as depicted in the Figures 7,8, 9 and 10. In the figure, the waved porous baffles provide considerable heat transfer enhancements in comparison with porous baffle and the average Nusselt number values for using porous baffles increase with the rise of Reynolds number. This is because the porous baffles interrupt the development of the boundary layer of the fluid flow and create the reverse/recirculating flow on the tip of porous baffles.

From Figure. 10 it can be seen that the friction factor and Nusselt number decreases with the increasing Reynolds number. When it compared with the rising height ratio, friction factor is started to reduce as shown in Figure. 10. The highest friction factor can be seen at ratio of Height $h/D_h=2/3$, as expected.

The decrease in pressure increases to a maximum with an increase in the pore density of aluminum at 40 PPI with the highest value of the pressure drop but for the waved porous baffles the pressure drop decreases by 2.4% by the transverse baffles. The pressure drop decreased due to the shape of the proposed porous baffle.

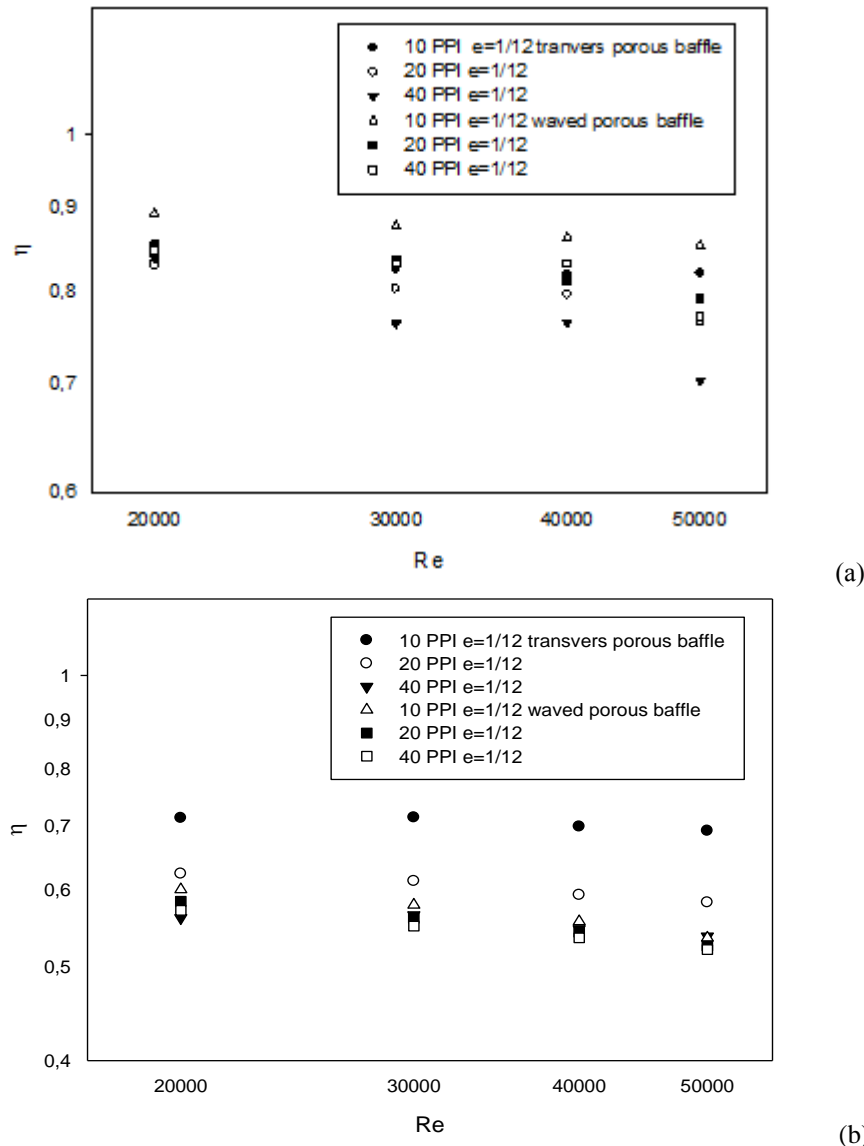


Figure 12. Thermal efficiency of the ratio with the Reynolds number for (a) $h/D_h = 1/3$ and (b) $h/D_h = 2/3$

For a fixed flow rate, if the pressure drop across the fins is large, then the effect of the permeability is low. On the other hand, when the flow rate is low and the pressure drop across the fins is small, the effect of the permeability is great.

Efficiency analysis is a step to optimize the implementation, choosing the best local conditions. The best improvement ratios of 0,8935 and 0,7134 on $h / D_h = 1/3$, $Re = 20000$, 10 PPI for porous corrugated baffles and $h / D_h = 2/3$, $Re = 30000$, 10 PPI for porous transverse baffles. The proposed porous baffle always remains effective and very important by bringing in the porous baffles of Kang-Hoon Ko, N. K. an improvement of the system says an improvement on the loss of load at the outlet of the rectangular channel equipped with waved porous baffles. The selected sample gives a good thermal efficiency of the system.

CONCLUSION

In this study, the effect of waved porous baffles which are attached to the inner surface of a rectangular conduct is numerically examined for steady-state 3D turbulent flow under constant heat flux boundary condition. the waved porous baffles are attached inside pipe. The parameters examined are the height distance porous baffles, thickness porous baffle, and Reynolds number. Numerical study has been carried out for the ratio of the waved porous baffle height to the rectangular pipe in the range of $h/D_h = 1/3$ and $2/3$, thickness porous baffle of $e = 0.00635$ and 0.0254 m, Reynolds number of $Re = 2 \times 10^4$ to 5×10^4 , and Prandtl number of $Pr = 0.71$. The values of fully developed Nusselt numbers and friction factors obtained in the present study for pipe with porous baffle are compared to those given in the literature to validate the accuracy of the turbulence model and numerical method. It is seen that heat transfer and pressure losses are higher for pipes with baffles.

It is also seen that heat transfer, pressure loss, and thermal performance factor for a pipe with porous baffles depend on the Reynolds number, geometry porous baffle, height porous baffles and thickness porous baffles. The use of solid baffles results in a heat transfer increment as high with the heat transfer in the rectangular conduct with porous baffle. It is also seen that heat transfer increases with increasing Reynolds number and height porous baffle in the range studied. Maximum and minimum heat transfers are obtained at for all pipe distance.

Friction factor increases with increasing Reynolds number except the waved baffle for which friction factor decreases due to decrease in friction losses, and friction factor decreases with height increasing porous baffle in the range studied. pipes with porous baffle, give maximum and minimum pressure losses for all rectangular conducts.

It is seen that pressure factor decreases with decreases the height porous baffle but increases with increasing number Reynold in the range studied. while minimum thermal performance factor is obtained at waved baffle. It is also seen that after a certain module, the flow characteristics indicate periodically repeating behavior.

NOMENCLATURE

| | |
|-------------------|---|
| c_1, c_2 | turbulent constant |
| C | inertia factor |
| d_p | Particle diameter |
| D_h | Hydraulic diameter hydraulique |
| f | friction factor |
| H | Heigtht channel |
| h | baffle height |
| I | turbulenceintensity |
| k_d | Stagnant conductivity |
| k_e | effective thermal conductivity of the porous baffle |
| k_f | thermal conductivity of the fluid |
| k_t | thermal dispersion conductivity |
| K_p | permeability |
| k | turbulent kineticenergy |
| \overline{Nu} | Averaged Nusselt number for baffled channel flow |
| \overline{Nu}_s | Averaged Nusselt number for the smooth channel |
| P | Pressure |

| | |
|---------------------------------------|--|
| R_e | Reynolds number |
| S | baffle spacing |
| S_ϕ | Source term |
| T | temperature |
| T_{in} | temperature inlet |
| U_{in} | Inlet velocity |
| u | velocity in the x direction |
| v | velocity in the y direction |
| ϕ | transported scalar |
| ρ | density |
| μ_t, μ_e, μ_l | laminar, turbulent and effective viscosity |
| $\sigma_k, \sigma_\epsilon, \sigma_T$ | $k - \epsilon$ turbulence model constant of k , ϵ and T |
| ϵ | porosity |
| α_p | thermal diffusivity of porous media |
| ϵ | Turbulent energy dissipation rate |
| f | external flow field |
| p | porous media |

REFERENCES

- [1] Cengel, Y. A., Ghajar, A. J., "Heat and Mass Transfer Fundamentals and Applications", McGraw Hill, New York, USA, book 2011.
- [2] Yue-Tzu Yang, Chih-Zong Hwang., "Turbulent Heat Transfer and Fluid Flow in a Porous-Baffled Channel", International Journal of Heat and Mass Transfer, 771–780, 2003.
- [3] B. Nicolau. Santos and J. S. Marcelode Lemos., "Flow and Heat Transfer in a parallel-plate channel with porous and Solid baffles" Numerical Heat Transfer, Part A, 49: 1–24, 2006.
- [4] Kang-Hoon Ko, Anand, N.K." Use of porous baffles to enhance heat transfer in a rectangular channel" International Journal of Heat and Mass Transfer 46:4191-4199. 2003.
- [5] Yu, Q., Thompson, B. E., Straatman, A. G.A," Unit Cube-Based Model for Heat Transfer and Fluid Flow in Porous Carbon Foam" Journal of Heat Transfer (2006).
- [6] N. Targui, H. Kahalerras, "Analysis of fluid flow and heat transfer in a double pipe heat exchanger with porous structures" Energy Conversion and Management,49:2008, 3217-3229, 2008.
- [7] P. C. Huang and K. Vafai "flow and heat transfer control over an external surface using a porous block array arrangement" Heat Mass Transfer, 31:1019-4030,1993.
- [8] H. Benzenine et al, "Numerical study on turbulent flow forced-convection heat transfer for air in a channel with waved fins" Mechanics,19:1392 – 1207,2013.
- [9] A. Tandiroglu, T. Ayhan, "Energy Dissipation Analysis of Transient Heat Transfer for Turbulent Flow in a Circular Tube with Baffle Inserts" Applied Thermal Engineering, 26:178-185 2006.
- [10] J. M. Choi, N. K. Anand, S. C. Lau, and R. T. Kukreja, "Heat (Mass) Transfer in a Serpentine Channel with Right-Angled Turns", Journal of Heat Transfer Transactions of the ASME 118 211-213,1996.
- [11] J. Bear," Dynamics of Fluids in Porous Media", American Elsevier Pub. Co., New York, 1972.
- [12] D. A. Nield, and A. Bejan, "Convection in Porous Media", Springer-Verlag, NewYork, 1992.
- [13] R. A. Wooding," Steady State Free Thermal Convection of Liquid in a Saturated Permeable Medium" Journal of Fluid Mechanics 2 :273-285 ,1957.
- [14] K. Vafai, and C. L. Tien, "Boundary and Inertia Effects on Flow and Heat-Transfer in Porous-Media" International Journal of Heat and Mass Transfer 24 :195-203,1981.
- [15] J. C. Slattery, "Flow of Viscoelastic Fluids Through Porous Media", AIChE J. 13:1066-1071,1967.
- [16] Slattery, J. C., Multiphase Viscoelastic Flow Through Porous Media, AIChE J. 14 :50-56, 1968.
- [17] M. L. Hunt and C. L. Tien," Non-Darcian Convection in Cylindrical Packed- Beds" Journal of Heat Transfer Transactions of the ASME 110 :378-384,1988.
- [18] A. Nakayama," PC-aided Numerical Heat Transfer and Convective Flow" CRC Press, Boca Raton, 1995.
- [19] O. Keklikcioglu.et al. "A cfd based Thermo Hydraulic Performance Analysis in a tube fitted with Stepped conical nozzle Turbulators" Journal of Thermal Engineering, Istanbul, 2:913-920, 2016.

- [20] O. Turgut and E. Kizilirmak, "Effects of Reynolds Number, Baffle Angle, and Baffle Distance on 3d Turbulent Flow and Heat Transfer in a Circular pipe", *Thermal Science*, 19: 1633-1648, 2015.
- [21] Ansys Inc. *Fluent 12.0 User's Guide*, Lebanon, USA, 2008.